Basis Set, Level, and Continuum Solvation Effects on the Stability of a Synthetic Dipeptide: PIDOTIMOD

Giuliano Alagona,*,† Caterina Ghio,† and Vincenzo Villani‡

CNR-ICQEM, Institute of Quantum Chemistry and Molecular Energetics, Via Risorgimento 35, I-56126 Pisa, Italy, and Dipartimento di Chimica, Università della Basilicata, Via N. Sauro 85, I-85100 Potenza, Italy

The conformational preferences of PIDOTIMOD, namely 3-(5-oxo-L-propyl)-L-thiazolidin-4-carboxyl acid, a synthetic dipeptide showing a beneficial influence on some immune functions both in mammalians and in humans, have been searched by varying two of its rotatable dihedral angles. Preliminary results in vacuo on the conjugated basis used the STO-3G* basis set. At that level, the ϕ_1, ϕ_3 potential energy surfaces for ϕ_2 equal either to 0° or 180° were also explored in the flexible rotor approximation. When ϕ_2 is equal to 180°, however, for $120° \leq \phi_1 \leq 260°$ the nitrogen proton shuttling to the adjacent carboxyl anion was observed; therefore, a constraint had to be imposed on the N−H bond distance to prevent this artifact. In the $\phi_2 = 180°$ potential energy surface computed employing the 6-31G* basis set, in fact, the proton remained on the N atom everywhere. The proton transfer was then studied in vacuo at the HF/6-31G* and 6-31+G* levels and, in contrast to the STO-3G* spontaneous process, the energy barrier turned out to be about 13 kcal/mol. The energy of selected conformers corresponding to minima on the potential energy surface in vacuo was computed with the inclusion of correlation corrections at the MP2 level and in aqueous solution in the polarizable continuum model framework. A sensitive influence of correlation effects on the trans forms with intramolecular H-bonds is observed, while the solvent stabilizes the conformer with the polar groups widely exposed to it. The energy gap among the cis rotamers amounts to ∼3 kcal/mol, with the energy of the most stable of them in vacuo ∼6 kcal/mol higher than that of the trans conformers. The most stable cis structure becomes the second most populated conformer in aqueous solution at the MP2 level, though all the cis conformers are sharply stabilized in solution. A preliminary study in vacuo of the trans−cis interconversion was also carried out.

Introduction

PIDOTIMOD (3-(5-oxo-L-prolyl)-L-thiazolidine-4-carboxylic acid) is a synthetic dipeptide which shows a positive effect on immune functions both in mammalians and in humans; it induces, in fact, the functional activation of the Interleukin-2 (IL-2) receptor located on the cell surface of T-lymphocytes stimulated by an antigen.[1] IL-2 is the T Cell Growth Factor and its receptor complex is constituted of a 75 kDa β-chain and a 55 kDa α-chain, which separately bind the IL-2 molecule. The interaction between IL-2 and the larger protein tells T-lymphocyte to proliferate and develops the antigen-specific clone.[2,3] PIDOTIMOD is an agonist of the IL-2 receptor and can play a major role as an immunomodulatory factor.[1]

The features and the conformational behavior of PIDOTIMOD (as its conjugate base, the "all-trans" conformer is displayed in Scheme 1) have been previously studied both theoretically, either by molecular mechanics (MM), normal mode vibrational analysis and dynamics,[4] or molecular dynamics (MD) simulations,[5] and experimentally by NMR spectroscopy.[4]

Through NMR measurements, performed in D$_2$O at 21 °C and pH = 7.0, where because of PIDOTIMOD's low pK_a (3.03) the conjugate base largely predominates, two classes of conformers, trans and cis around the peptide bond between the rings

SCHEME 1

$\phi_1 = N_6CCO$

$\phi_2 = OCNC_5$

$\phi_3 = O_8CCN$
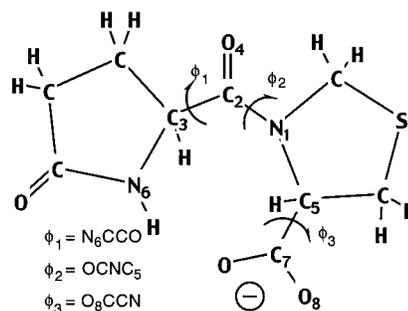
(ϕ_2 in Scheme 1), with relative populations of 0.55 and 0.45, respectively, were observed.

Through MM, a good agreement with the experimental data was obtained when the shielding solvent effects were mimicked using a relative permittivity $\epsilon = 7$. Five nonequivalent conformers were determined.[4] From a vibrational viewpoint, the molecule appeared to be rather rigid with some correlated motions inside the rings.

Through MD simulations at 300 K, only one cis and two trans conformers, all hardly flexible, were found to be stable, while two puckered forms in rapid interconversion of the oxoprolyl ring were detected.[5] At even slightly higher temperatures, the trans conformers resulted to be thermally mixed as in the case of the cis conformers.[5]

* Corresponding author. E-mail: G.Alagona@icqem.pi.cnr.it. Fax: ++39-050-502270.
† Institute of Quantum Chemistry and Molecular Energetics.
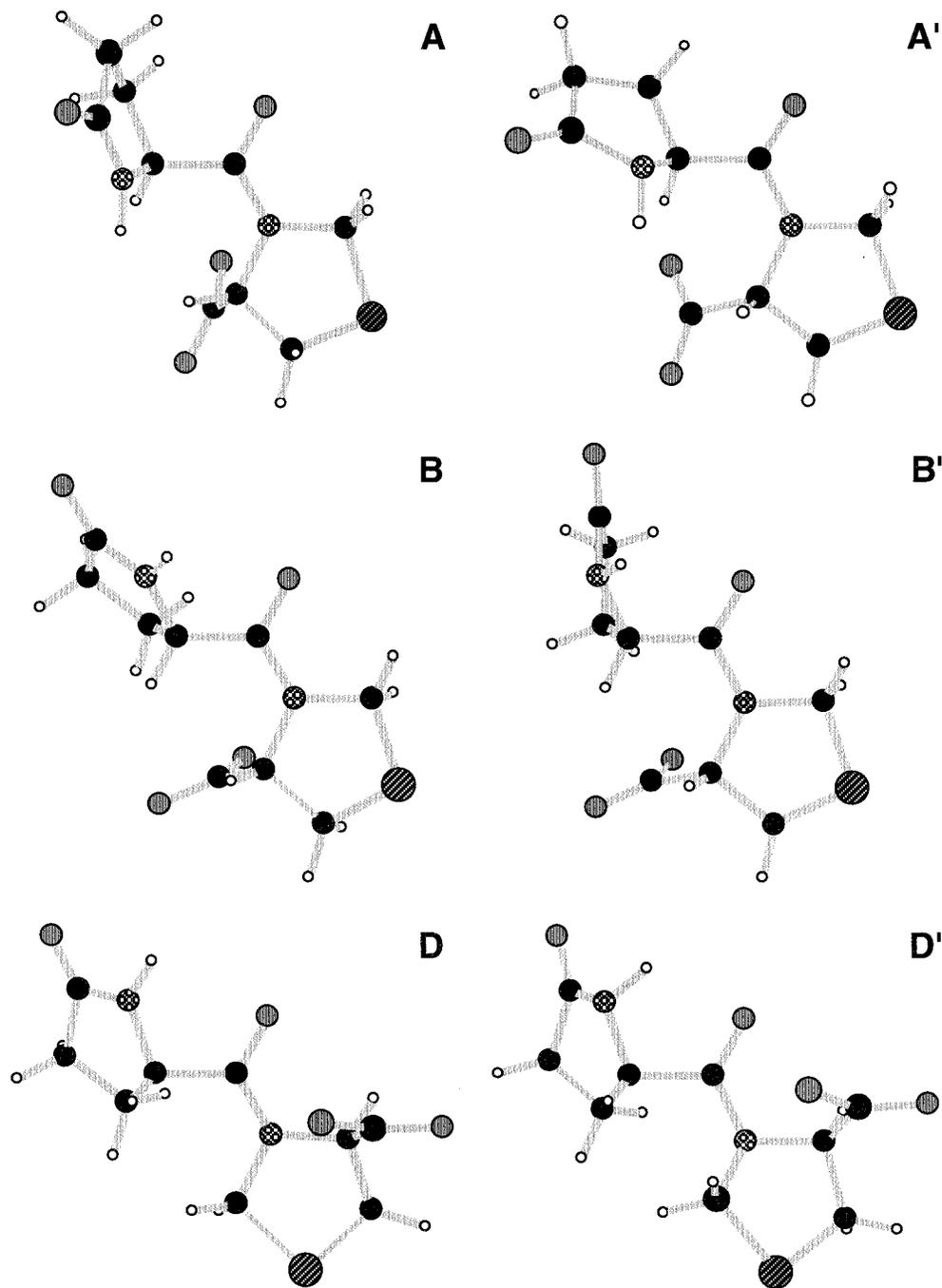‡ Università della Basilicata.

Figure 1. PIDOTIMOD structures optimized with MM (left-hand side) and at the HF/STO-3G* level (right-hand side) keeping rigid the three main dihedral angles to their MM values. Trans structures: A, A′ (upper part) and B, B′ (middle part). Cis structures: D, D′ (lower part).

An invariant molecular shape elongated with an almost perpendicular orientation of the rings was found in all cases,[4] and the authors suggested that this moiety might play a key role in the biological activity.

In the present paper, the ab initio results either in vacuo or in solution are compared to those obtained with MM simulations in a previous work,[4] in order to check their reliability. Therefore, the ab initio conformational study was carried out on a grid for couples of values of the dihedral angles ϕ_1 and ϕ_3 (see Scheme 1 for their definition) with basis sets of increasing quality in vacuo. The calculations were performed using the conjugated base, which should be the bioactive form, in place of the acid for the reasons put forward above. The main difference among the basis sets was found in the map region where the −NH group faces the −COO$^-$ group, because at the STO-3G* level

the proton moved from nitrogen to carboxylate with a noticeable energy gain. The calculations in aqueous solution with the solvent described as a dielectric medium in the framework of the polarizable continuum model (PCM) were carried out on the in vacuo optimized conformers to evaluate their relative stability.

Computational Details

All the calculations were performed using the Gaussian 94[6] system of programs, running on the IBM-RISCs 6000-590 at ICQEM (Pisa), with the inclusion of modified versions of the l502 and l702 links. Details of the computational methods, when necessary, are given in the relevant sections.

Choice of the Basis Set. The energies of the three most stable structures (one cis, D, and two trans, A and B, forms; see Figure 1, left-hand side), obtained from MM simulations in vacuo

Stability of a Synthetic Dipeptide: PIDOTIMOD

J. Phys. Chem. A, Vol. 103, No. 29, 1999 **5825**

TABLE 1: MM and ab Initio Relative Energies in kcal/mol of the B and D Type Structures with Respect to the A Type, Taken as Zero

	ΔE AMBER[a]	ΔE^b STO-3G*	ΔE^b 6-31G*	$\Delta G_{SCF}{}^b$ STO-3G*	$G^{sol\ b}$ STO-3G*
A	0.	0.	0.	0.	−63.98
B	0.84	−0.64	−2.32	0.13	−63.20
D	3.79	5.24	7.99	−1.18	−70.39
A′	0.	0.		0.	−54.30
B′	0.84	2.98		−1.60	−58.88
D′	3.79	7.24		−0.42	−61.96
A″	0.	0.		0.	−55.37
B″	0.67	0.99		−0.29	−56.64
D″	0.54	9.86		3.04	−62.19

[a] From ref 4. [b] Rigid MM geometries[a] were used for A, B, and D. The A′, B′, and D′ and A″, B″, and D″ structures have been relaxed in vacuo while keeping only the main dihedral angles (see text) at their $\epsilon = 1$ and $\epsilon = 7$ MM values, respectively.

($\epsilon = 1$),[4] were evaluated ab initio via single-point calculations employing the STO-3G*[7] (i.e., the STO-3G[8] basis with a set of d functions added to sulfur) and 6-31G*[9,10] basis sets. According to the results obtained by Alkorta,[11] who compared the description of the geometric and electronic properties in several sulfur derivatives given by different methods and basis sets, both the STO-3G* and 6-31G* basis sets produce good results for bond lengths and bond angles. Especially the latter basis set is to be considered an adequate choice for geometry optimizations of systems containing sulfur atoms, though satisfactory electronic properties (measured through dipole moments[11]) could be obtained only with the inclusion of correlation effects at the second-order Møller−Plesset (MP2) perturbation level,[12] which is, however, beyond our computer capabilities for a system of this size. Thus, single-point MP2 calculations have been carried out, where necessary.

The relative energies at the various levels are reported in Table 1. Notice that the ordering of the energies is not univocally determined. Interestingly enough, the STO-3G* basis set shows a trend analogous to the 6-31G* one, though slightly damped. Therefore, the STO-3G* basis set was preliminarily used to optimize the geometries of the three conformers and to compute the solvent effect, G^{sol}. For a brief description of the computational method, refer to the relevant section. However, the use of this basis set is not recommended for charged systems with intramolecular H-bonds because of the major flaw revealed in the analysis of the potential energy surfaces.

As can be seen by comparing the starting geometries, which correspond to the minima located with MM, i.e., A ($\phi_1 = -100.30°$, $\phi_2 = -179.80°$, $\phi_3 = -1.99°$), B ($\phi_1 = -35.77°$, $\phi_2 = -179.88°$, $\phi_3 = 47.07°$), and D ($\phi_1 = -5.81°$, $\phi_2 = 8.80°$, $\phi_3 = 3.71°$),[4] displayed in Figure 1 (left-hand side) and the structures hence derived after optimization at the HF/STO-3G* level of all the other parameters to relieve structure strains, namely A′, B′, and D′, also displayed in Figure 1 (right-hand side), there is a satisfactory agreement between the MM and ab initio results, even as far as the energy ordering is concerned.

MM minimizations "in solution", i.e., using as dielectric constant $\epsilon = 7$, moreover, produced a preferential stabilization of D″ ($\phi_1 = -7.57°$, $\phi_2 = 47.78°$, $\phi_3 = 26.78°$) with respect to A″ ($\phi_1 = -100.09°$, $\phi_2 = 179.18°$, $\phi_3 = 10.20°$) and B″ ($\phi_1 = -29.23°$, $\phi_2 = -159.33°$, $\phi_3 = 41.02°$),[4] even though A″ remained the most stable one, as shown in Table 1. The ab initio solvent effect is also much more favorable for the structures of D type than for the others, but the agreement with the MM values is limited to this result. We were interested, however, in

TABLE 2: Local Minima Found in Vacuo on the HF/6-31G* $\phi_2 = 0°$ and $\phi_2 = 180°$ Conformational Maps with Their Relative Energies and Free Energies (kcal/mol) with Respect to Ta, Taken as Zero,[a] and the Corresponding Torsional Angles

name	ΔE	ΔG^v	ϕ_1	ϕ_2	ϕ_3
Ta	0.	0.	311.55	180	188.48
Tb	0.25	0.47	357.18	180	177.79
Tc	0.56	1.62	230.44	180	228.79
Td	0.63	0.76	308.99	180	164.58
Te	0.99	1.53	161.60	180	137.34
Ca	6.13	6.20	348.67	0	173.10
Cb[b]	7.28	8.47	253.59	0	171.95
Cc	9.43	9.56	136.68	0	172.45

[a] The reference value is $E_{SCF} = -1153.166322$ hartrees. [b] Structure with an imaginary frequency.

assessing whether the MM-determined minimum structures were reliable or not.

Results and Discussion

To compare stable ab initio structures to the MM ones, the whole potential energy surfaces (PES) for $\phi_2 = 0°$ (cis) and $\phi_2 = 180°$ (trans) were computed at the STO-3G* level. In the trans conformations ($\phi_2 = 180°$), however, when the polar H faces the carboxyl group (roughly for $120° < \phi_1 < 260°$) the proton moves spontaneously from the N atom to one of the carboxyl oxygens. Therefore, to maintain the carboxylate ionized structure, the NH distance was constrained to 1.03 Å in the aforementioned region.

The lowest minimum found for the cis structure is in good agreement with D (i.e. it is close to $\phi_1 = \phi_2 = \phi_3 = 0°$), while for the trans conformers the ab initio lowest minimum is found at about $\phi_1 = 150°$, $\phi_3 = 120°$, to be compared with $\phi_1 = 260°$, $\phi_3 = 0°$ (A) and $\phi_1 = 324°$, $\phi_3 = 48°$ (B).

The ab initio STO-3G* minimum, however, is about 16 kcal/mol more stable than the MM ones, but this fact (as the proton shuttling as well) could be an artifact of the minimal basis set, which is known to overestimate the strength of H-bonds and favor too short separations.[13] Moreover, the calculations are carried out in vacuo; in the presence of the solvent the proton transfer may be forbidden or a structure without intramolecular H-bonds may be sharply stabilized, thus preventing the possibility of close contacts between the solute polar groups.

To better clarify the gas-phase behavior of PIDOTIMOD, the $\phi_2 = 0°$ and $\phi_2 = 180°$ PES were computed again using the 6-31G* basis set, which is still affordable, though extremely expensive, for this system in the flexible rotor approximation (with the exception of the C−H bond distances, kept at 1.09 Å, and the COO− group, which was kept planar throughout). The minima, listed in Table 2 with the indication of their relative energies, locations, and given names, have been checked performing frequency calculations. None of them produced any imaginary frequency but Cb, which has an imaginary frequency because, when $\phi_2 = 0°$, it is probably a transition state. The frequency calculations allowed us to evaluate the internal free energy, also reported in Table 2, of these structures.

The intramolecular free energy in vacuo, G^v ($T = 298$ K, $p = 1$ atm), is computed in the rigid-rotor harmonic oscillator approximation,[14] by adding G_{intra} to the internal energy,

$$G_{intra}(T,p) = 0.9\text{ZPE} + \Delta H(0-T) - T\Delta S(0-T) \quad (1)$$

ZPE is the vibrational energy at 0 K, while $\Delta H(0-T)$ and $\Delta S(0-T)$ stand for the changes in enthalpy and entropy between
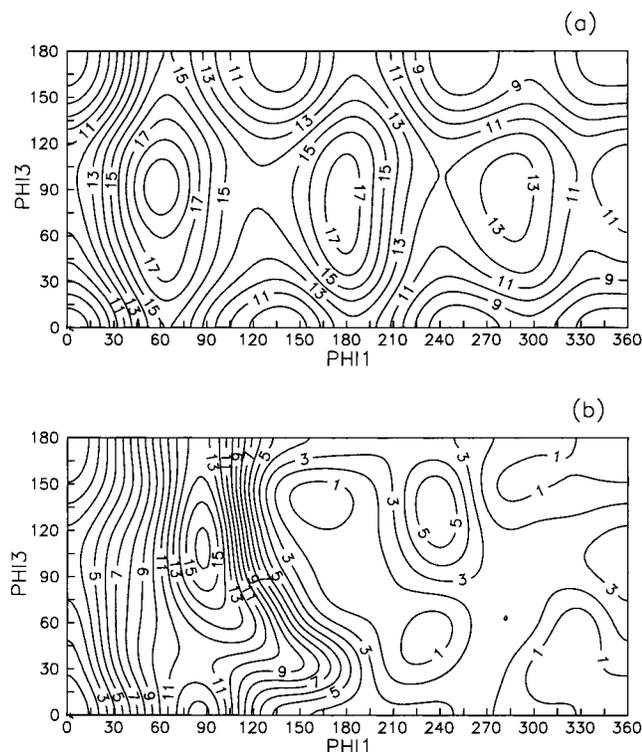
5826 *J. Phys. Chem. A, Vol. 103, No. 29, 1999*

Alagona et al.

Figure 2. ϕ_1, ϕ_3 conformational maps computed at the HF/6-31G* level (a) for $\phi_2 = 0°$ and (b) for $\phi_2 = 180°$ (isopotential lines spaced by 1 kcal/mol).

0 and 298 K. A scaling factor of 0.9 was applied due to the known overestimate of vibrational frequencies at the HF/6-31G* level.[15]

The trend of the $\phi_2 = 0°$ surfaces is analogous with either basis set, though the STO-3G* one is much higher and somewhat steeper than the 6-31G* surface, shown in Figure 2a. This is a feature of the 6-31G* basis set observed in the conformational map of 1,2-ethanediol[16] even in comparison with the 4-31G basis set.[17] The 6-31G* minimum found for the cis structure, Ca, located at $\phi_1 = 348.7°$, $\phi_3 = 173.1°$, in the upper right corner of the map in Figure 2a, is still close to $\phi_1 = \phi_2 = \phi_3 = 0°$, while the minimum trans conformer, Ta, is found at $\phi_1 = 311.6°$, $\phi_3 = 8.48°$ (to be compared with $\phi_1 = 260°$, $\phi_3 = 0°$ (A) or $\phi_1 = 324°$, $\phi_3 = 48°$ (B)), as can be seen by examining the trans conformational map, displayed in Figure 2b. This surface is also smoother than the STO-3G* one, but the main difference is that at the 6-31G* level the proton shuttling does not occur. Moreover, at the HF/STO-3G* level, even forcing the proton to stay on the N atom, the strength of the H-bond with the carboxyl oxygen is noticeably enhanced, thus producing an overestimate of the stability of the structures with $120° \leq \phi_1 \leq 260°$, as can be inferred from the large energy differences on the STO-3G* surface, which are more than twice as much as those of the 6-31G* one.

To shed some light on this mechanism, the proton transfer was studied at the 6-31G* level starting from the structure Te which presents the two partners close enough. The proton was then moved along the line joining nitrogen to the carboxyl oxygen, allowing the structure to relax, apart from the afore-mentioned exceptions. Only when the O···H distance becomes decidedly shorter than 1.4 Å does the N—H bond start lengthening sensitively, while the barrier turns out to be about 13 kcal/mol (Figure 3a). The energy profile is of course opposite using the STO-3G* basis set (Figure 3b), but not even a local minimum is found for the proton bound to the N atom. The
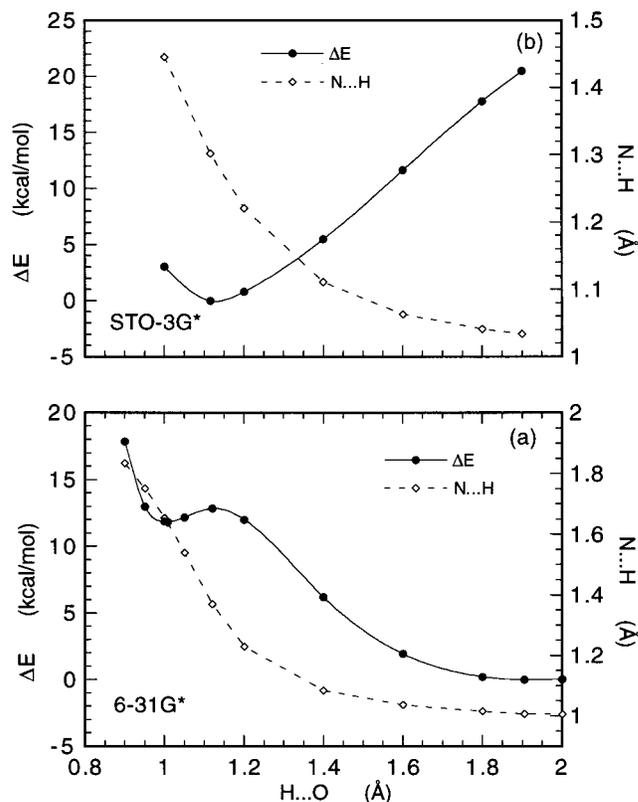

Figure 3. Energy profile for the proton transfer along the H···O separation at the (a) HF/6-31G* and (b) STO-3G* levels. The corresponding change in the N—H distance is also shown.

STO-3G* behavior was somewhat amazing, because we never found anything like that in our studies on H-bonded dimers,[18] even in the case of anion interactions with water.[19] Therefore, we decided to better analyze this particular type of reaction, i.e., the proton transfer between H-bonded partners, which was the object of several previous studies[20,21] even in solution (see ref 22 and references therein), using two different model systems: the carboxylate anion and ammonia or formamide. At the STO-3G level, the stable adduct between ammonia and HCOO⁻ presents a short H-bond (1.45 Å) between NH and one of the carboxyl oxygens, as expected. On the contrary, in the adduct between formamide and HCOO⁻, the proton is closer to one of the carboxyl oxygens (1.17 Å) than to the N atom (1.24 Å). Both distances, however, are larger than in a normal covalent bond. Therefore, at the STO-3G level, the change in the N hybridization produced by its involvement in a peptide bond is sufficient to give rise to the proton shuttling from nitrogen to one of the carboxyl oxygens. Because of the presence of the anion, both model systems have also been considered with a basis set including sp diffuse functions[23] at the MP2/6-31+G*//HF/6-31+G* level as well, i.e., using the HF/6-31+G* geometries of the partners fully optimized for increasing separations of the proton from its N. In the calculations also the N···O distance was allowed to relax. The correlation effect, which produces a lowering in the energy profiles in the region 1.1 < N···H < 1.6 Å, is larger in percentage for formamide···HCOO⁻ than for ammonia···HCOO⁻. The regression coefficients of the lines obtained plotting the HF values vs the MP2 ones are 0.981 and 0.997, respectively. Neither at the MP2/6-31+G* level nor at the HF/6-31+G* level does the proton shuttling occur spontaneously, as expected, while the trend of the interaction energy, displayed in Figure 4, very steep for ammonia···HCOO⁻, decreases for formamide···HCOO⁻ to almost match the HF/6-31G* behavior of PIDOTIMOD (dotted
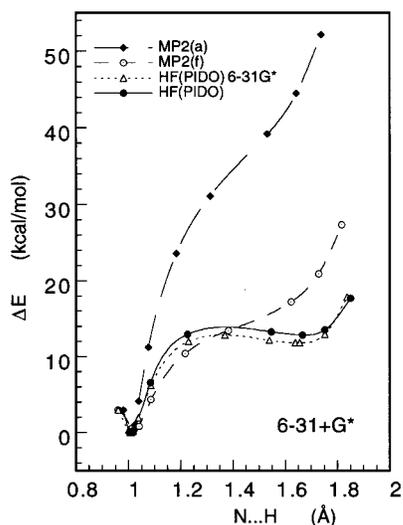
Stability of a Synthetic Dipeptide: PIDOTIMOD

J. Phys. Chem. A, Vol. 103, No. 29, 1999 **5827**

Figure 4. Energy profiles for the proton transfer along the N···H separation at the MP2/6-31+G*//HF/6-31+G* level for ammonia···HCOO⁻ (long dashes) and formamide···HCOO⁻ (short dashes). The corresponding profile at both the HF/6-31G* (dotted line) and 6-31+G* (solid line) levels for PIDOTIMOD is also shown.

line). This curve is fairly consistent with the results, even though computed at a few fixed O···N separations, obtained by Li et al.[21] in the study, among others, of proton transfer from imidazole to formate. To assess the basis set effect on the proton-transfer energetics, the reaction profile for various O···H separations was computed for PIDOTIMOD at the HF/6-31+G* level. These results, also reported in Figure 4 (solid line), are slightly less favorable than the 6-31G*, and by inference it is likely that the MP2 corrections would produce a sensitive lowering in the curves.

The problem of proton transfer is however a side issue with respect to this investigation, raised by the anomalous behavior of the STO-3G basis set.

The only consequence which is brought about by this fact is that it is convenient to use a classical method when an adequate quantum calculation is not affordable. We have also reached this conclusion studying π-stacked complexes,[24] where the inclusion of electron correlation at the MP2 level was needed to obtain reliable results, fairly comparable to the classical ones.

Correlation Effect. We have performed MP2 correlation corrections on the local minima found along the HF/6-31G* PES, because geometry optimizations at the MP2/6-31G* level are extremely demanding in terms of computer resources for PIDOTIMOD. The relative weight of correlation effects is however limited, stabilizing at most by about 2 kcal/mol the Tc and Te structures with respect to the Ta, Tb, and Td ones, whose stability is practically unaltered after the correlation corrections (see Figure 5a). Consequently, Tc and Te become the most stable conformers. As far as the cis structures are concerned, the MP2 correction stabilizes Cb and Cc much more than Ca, thus making Cb the most stable cis conformer. It is apparent from the structures reported in Figures 6 and 7 that the Tc and Te conformers show an intramolecular H-bond, while in Cb there is a favorable interaction between the prolyl NH group and one of the carboxyl oxygens, though not amenable to a strong H-bond. In Cc, the CH₂ group, activated by the adjacent S and N, faces the prolyl N lone pair. These kinds of interactions seem thus to be responsible for the increased weight of correlation corrections.

In the next section, the correlation correction to the relative energies of the various conformers in solution is also discussed.
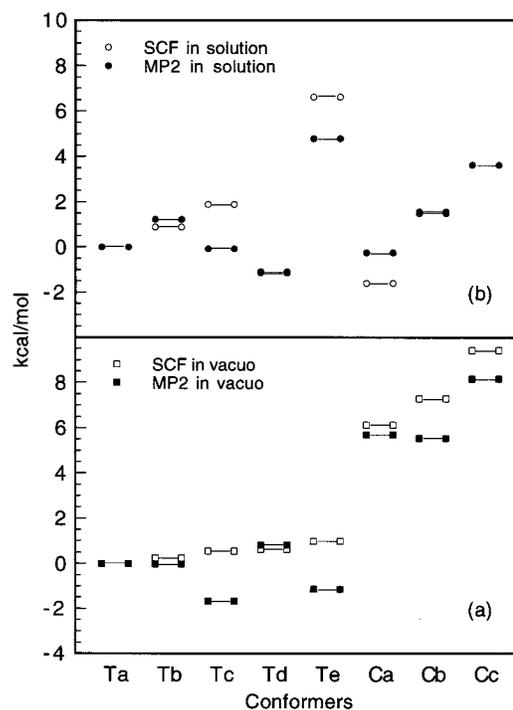

Figure 5. Relative energies in vacuo (a) and free energies in aqueous solution (b) in the PCM framework (see text) at the 6-31G*/HF (empty markers) and MP2 (solid markers) levels for the lowest energy conformers on the $\phi_2 = 0°$ and $\phi_2 = 180°$ PES with respect to Ta, taken as zero (the reference values in hartrees are $E_{SCF} = -1153.166322$, $G_{SCF} = -1153.279651$, $E_{MP2} = -1155.470548$, and $G_{MP2} = -1155.575864$).

Solvent Effect. The PCM approach, which accounts for the electrostatic effect felt by the wave function of a molecular solute M embedded in a continuum solvent of dielectric constant ϵ, is fairly well known to computational chemists. However, recent modifications introduced in the method suggest a need to describe it briefly, to show which algorithms have been used in the present work. More exhaustive descriptions can be found elsewhere,[25-27] with the caution that the changes quoted herein (embodied in Gaussian after the completion of this work) override the original implementation.

The Hamiltonian of the system is made up of two terms, one related to the unperturbed solute, $H°(M)$, and the other, V_σ, accounting for solute−solvent interaction:

$$(H°(M) + V_\sigma)\psi_M = E_M\psi_M \tag{2}$$

The solute is located in a cavity[25d,27] inside the dielectric medium shaped on the solute itself. A charge distribution appears on the cavity surface, produced by the solute total charge distribution (electrons and nuclei) and also by the polarization charges. These charges, used to polarize the solute charge distribution, are corrected for their mutual polarization and for the charge escaped outside the cavity. They consist of two sets depending on the solute electrons (e) and nuclei (N), respectively, computed exploiting linear equations in matrix form:[28]

$$q^e = AD^{-1}E_n^e; \quad q^N = AD^{-1}E_n^N \tag{3}$$

The elements of E_n^e and E_n^N are the normal components of the electric field, due to the solute electrons and nuclei, acting on the surface tiles; A is the diagonal matrix of the surface tile areas, while the elements of D depend only on ϵ and on the geometry of the tiles. In this formulation, coupling the boundary
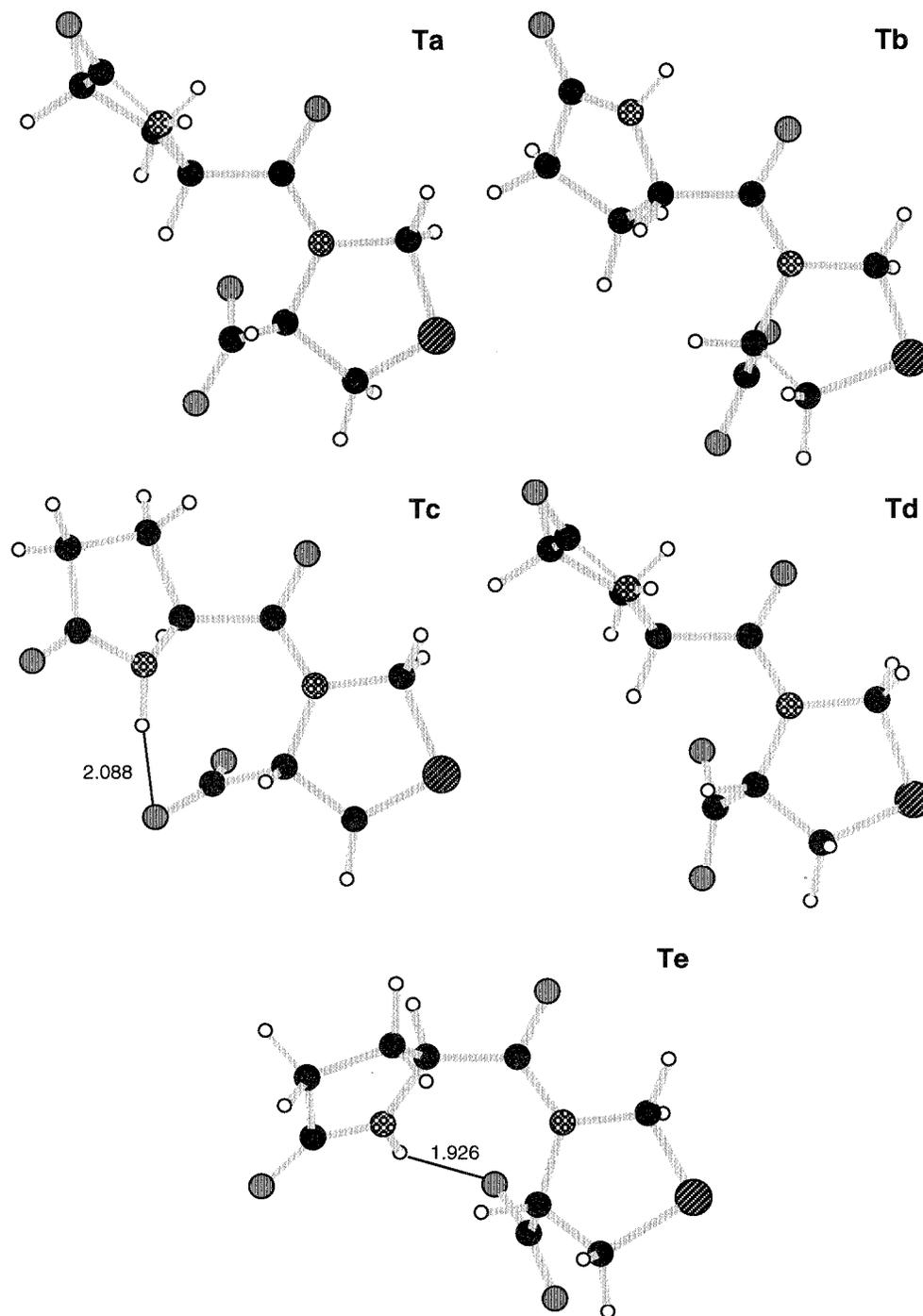
Ta

Tb

Tc

2.088

Td

Te

1.926

Figure 6. Structures corresponding to the minima on the HF/6-31G* potential energy surface for $\phi_2 = 180°$.

element method to solve the electrostatic problem to PCM for solvation, all the molecular properties are computed via a single SCF calculation, in place of the three needed in the original computer code.

To normalize the polarization charges appearing on the cavity surface, the procedure ICOMP=4 of PCM in Gaussian94[6] was used. The additional charges, which mimic the charges that should develop in the bulk of the dielectric medium as a reaction to the escaped electronic tails, are placed on the cavity surface and depend on the solute electronic density in each of its points.[29] The united atom topological model (UAHF) for the definition of the cavity[27] was also used because, optimizing the van der Waals radii for atoms and atomic groups, it produces

very accurate electrostatic solvation free energies, G_{el}:

$$G_{el}^{X} = E_{tot}^{X} - (1/2)\int \Gamma_M(\mathbf{r})V_\sigma(\mathbf{r})\, d\mathbf{r} \qquad (4)$$

where $E_{tot}^{X} = E_M^{X} + E^{nuc}$ [25c] and X stands either for HF or MP2.

The solvent effect at each level is therefore defined as

$$G_X^{sol} = G_{el}^{X} - E_X^{\circ} \qquad (5)$$

where E_X° is the energy of the solute in vacuo at the X level. The total molecular free energy in solution is obtained by considering also the effect of cavitation,[30] dispersion, and
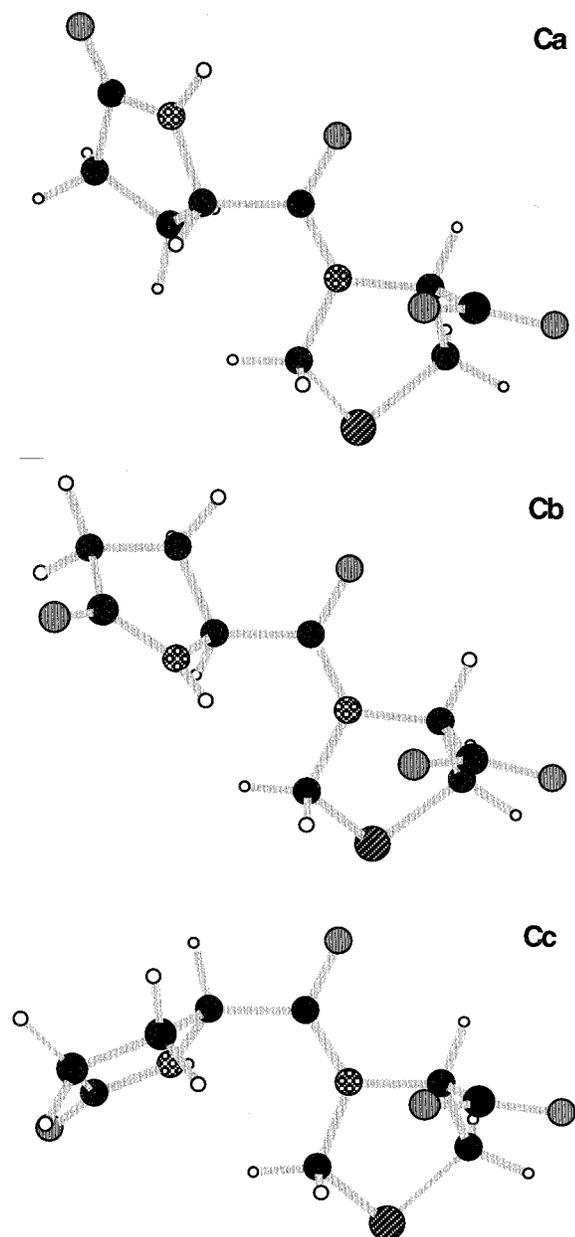
Stability of a Synthetic Dipeptide: PIDOTIMOD

J. Phys. Chem. A, Vol. 103, No. 29, 1999 **5829**

Ca

Cb

Cc

Figure 7. Structures corresponding to the local minima on the HF/6-31G* potential energy surface for $\phi_2 = 0°$.
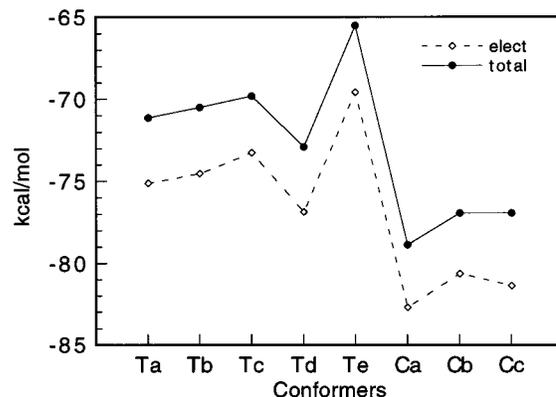

Figure 8. Electrostatic (diamond) and total (solid circle) solvent effect (G^{sol}) at the 6-31G*/HF level for the lowest energy conformers on the $\phi_2 = 0°$ and $\phi_2 = 180°$ PES.
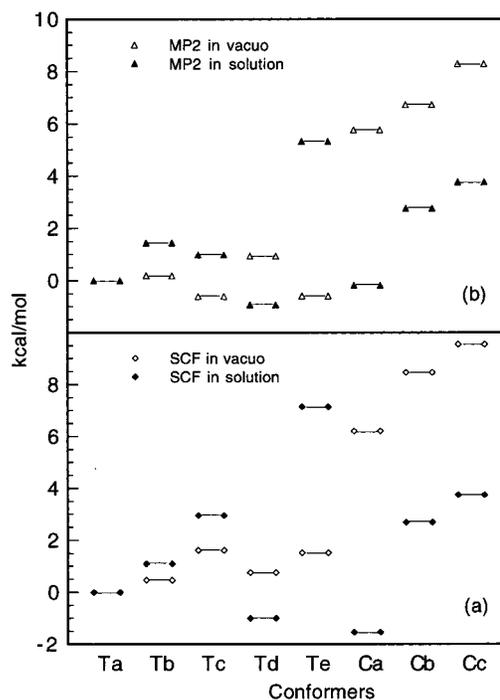

Figure 9. 6-31G* relative free energies (including G_{intra}, the intramolecular contribution computed in vacuo) in vacuo (empty markers) and in aqueous solution (solid markers) for the lowest energy conformers on the $\phi_2 = 0°$ and $\phi_2 = 180°$ PES with respect to Ta, taken as zero, (a) at the HF level (diamonds) and (b) at the MP2 level (triangles).

repulsion,[31] which is however limited to the energy. These contributions, called DCR for short, in fact do not affect the solute wave function, because they do not enter the Hamiltonian.

$$G_{tot}^X = G_{el}^X + G_{cav} + G_{dis} + G_{rep} \qquad (6)$$

In the following discussion, we are going to deal with the total solvent effect, unless otherwise specified. The total solvent effect actually differs by 3.4−4.4 kcal/mol, at most, from the electrostatic one, as shown in Figure 8. The cavitation term is in fact almost constant in this system, ranging from 27.2 (for Tc) to 27.9 kcal/mol (for Cc); moreover, the repulsion and cavitation contributions tend to counterbalance the dispersion one.

The correlation correction in solution is obtained while keeping the solvent frozen in its HF description, i.e., the polarization of the solvent is neglected at the correlated level.[32]

The 6-31G* relative free energies with respect to the Ta conformer, taken as zero, at the HF and MP2 levels in vacuo

and in solution are displayed in Figure 9, together with the differential solvent effect at both levels. Notice that both the in vacuo and in solution values include G_{intra}. This explains the difference in the relative values with respect to those reported in Figure 5, whereas the solvent effect remains unaltered.

The solvent effect is fairly strong, as expected for charged systems. The solvent stabilizing effect is sensitively larger for the conformers with the polar groups fully exposed to the solvent, such as the cis conformers (see Figure 7), than for those presenting either intramolecular H-bonds or less solvent accessible structures. Because of the small internal energy differences among the trans conformers at the SCF level, however, the solvation free energy trend is fairly close to the differential solvent effect.

The MP2 correlation effect stabilizes the conformers with intramolecular H-bonds also in solution, while Ca is less favorable after correlation corrections. The Ca conformer, the most stabilized by the solvent, in aqueous solution is ∼0.5 kcal/
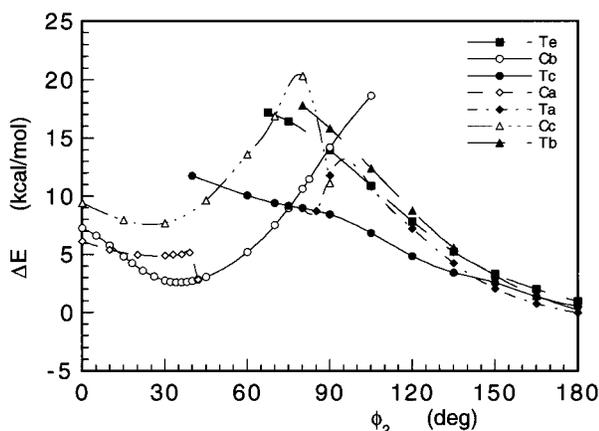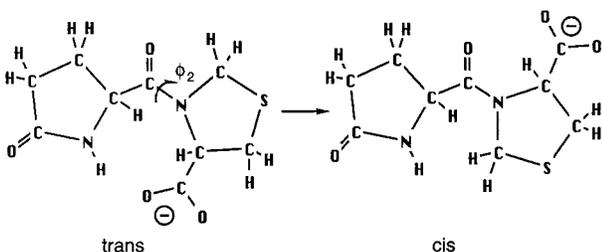
5830 *J. Phys. Chem. A, Vol. 103, No. 29, 1999*

Alagona et al.

Figure 10. Cis−trans interconversion profiles obtained starting from either the cis arrangements (empty markers) or the trans ones (solid markers).

SCHEME 2

mol more favorable than Td at the SCF level and just ∼0.8 kcal/mol less favorable than Td at the MP2 level (see also Figure 5b).

Interestingly enough, PCM calculations in solution stabilize considerably the cis forms, both at the SCF and MP2 levels.

If the thermal corrections to the Gibbs free energy computed in vacuo (G_{intra}) are added to the internal energies and to the solvation free energies, the plots, displayed in parts a and b of Figure 9, show a limited change (up to 0.26 kcal/mol) for Ta, Ca, Td, Cc, and Tb in increasing order, while the change is somewhat more sensitive for Te, Tc, and Cb (0.57, 1.04, and 1.13 kcal/mol, respectively).

Trans−Cis Interconversion. The rotation about the bridged peptide bond (see Scheme 2) was studied in vacuo starting from several either trans or cis low-energy structures, as shown in Figure 10, because only the $\phi_2 = 0°$ and $\phi_2 = 180°$ PES have been fully explored. The curve trend is due to the fact that the upper curves plunge into the lower ones upon inversion of the pyramidalization at the thiazolidin N atom. Of course, the curves correspond to different sections of the potential energy hypersurfaces.

This problem, however, is very demanding from both the computational and methodological points of view and cannot be addressed herein, in that it deserves a thorough examination. A preliminary analysis of the interconversion pathway, in the zone of the most favorable "crossing" between the two curve families, which occurs in the $\phi_2 = 75°$ region for $\Delta E \approx 9$ kcal/mol, was carried out. The path joining the two potential energy profiles, considered by computing a ϕ_1,ϕ_3 grid of points, is uphill with an additional barrier of about 8 kcal/mol, which produces a total barrier of ∼17 kcal/mol.

From the plots in Figure 10, it is apparent that the rotamers become more stable when ϕ_2 is about 30−40°. The origin of this peculiar feature was thus explored. Moreover, interestingly enough, in the $\phi_2 = 40°$ region, we located a transition state

TABLE 3: HF/6-31G* Minima Obtained in Vacuo by Relaxing ϕ_2 in the Cis and Trans Low-Energy Structures, with the Corresponding Torsional Angles, Relative Energies in Vacuo, Free Energies in Solution (kcal/mol) with Respect to Ta(opt), Taken as Zero,[a] and the Solvent Effect

name	ΔE	ΔG^v	ϕ_1	ϕ_2	ϕ_3	G^{sol}	ΔG_{tot}
Ta(opt)	0	0	301.80	194.56	183.06	−69.88	0
Tb(opt)	0.03	0.30	348.89	195.84	176.09	−70.16	−0.25
Tc(opt)	0.74	1.60	222.41	188.79	47.01	−67.83	2.79
Td(opt)	0.26	0.39	296.53	200.55	160.52	−69.47	0.67
Te(opt)	0.52	1.23	154.71	200.90	140.53	−66.40	4.01
Ca(opt)	5.25	5.42	344.22	26.69	171.28	−75.11	0.02
Cb(opt)	2.95	3.91	271.48	35.57	171.00	−69.95	2.88
Cc(opt)	7.93	8.41	139.03	24.67	171.60	−73.32	4.49

[a] The reference values are $E_{SCF} = -1153.166871$ hartrees, $G_{SCF} = -1153.278235$ hartrees.
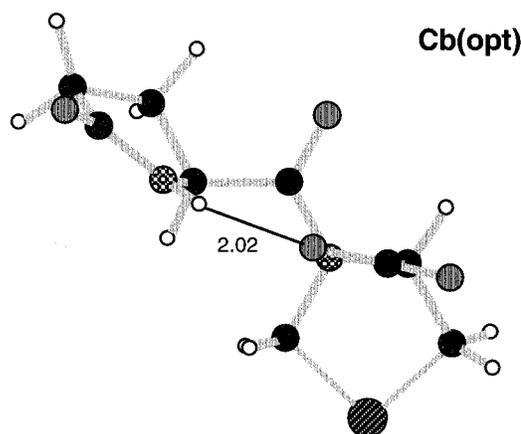

Figure 11. Structure of Cb(opt) obtained starting from Cb and relaxing also ϕ_2 at the HF/6-31G* level.

with a barrier (∼13 kcal/mol), considerably more favorable than that found at $\phi_2 = 75°$.

Low-Energy Structures with ϕ_2 Different from 0° or 180°. Other structures with intermediate values of ϕ_2, besides the purely trans and cis ones are stable in the flexible rotor approximation. This is probably due to the fact that neither Ca or Ta is the lowest energy structure though all the structures considered above are local minima, apart from Cb. By optimizing the geometries in vacuo at the HF/6-31G* level, after removing the constraint on ϕ_2, starting from the $\phi_2 = 0°$ lowest energy conformers, Cb(opt) becomes the most stable cis ($\phi_2 = 35.6°$) structure in vacuo, only 2.61 kcal/mol higher in energy than Ta, because of the H-bond between the prolyl ring N hydrogen and one of the carboxyl oxygens, which can be established for that value of ϕ_2. On the contrary, starting from the $\phi_2 = 180°$ lowest energy conformers, after full optimization in vacuo at the HF/6-31G* level, the most stable trans ($\phi_2 = 194.6°$) structure, Ta(opt), is only ∼0.3 kcal/mol more favorable than Ta.

The relative stabilities in vacuo and in solution, computed for all the structures optimized in vacuo at the HF/6-31G* level, are reported in Table 3 together with the optimized torsional angles and the relevant solvent effect. The geometrical features of the fully optimized structures, however, are hardly distinguishable from the starting structures (that were optimized by keeping ϕ_2 fixed at 0° or 180°) with the exception of Cb(opt), which is thus displayed in Figure 11. Despite the less stabilizing solvent effect felt by Cb(opt) with respect to Cb (−69.9 vs −76.9 kcal/mol), the Cb(opt) relative free energy is only 2.9 kcal/mol less favorable than the Ca(opt) one at the SCF level (0.6 kcal/mol at the MP2 level), while Cb was 3.1 kcal/mol
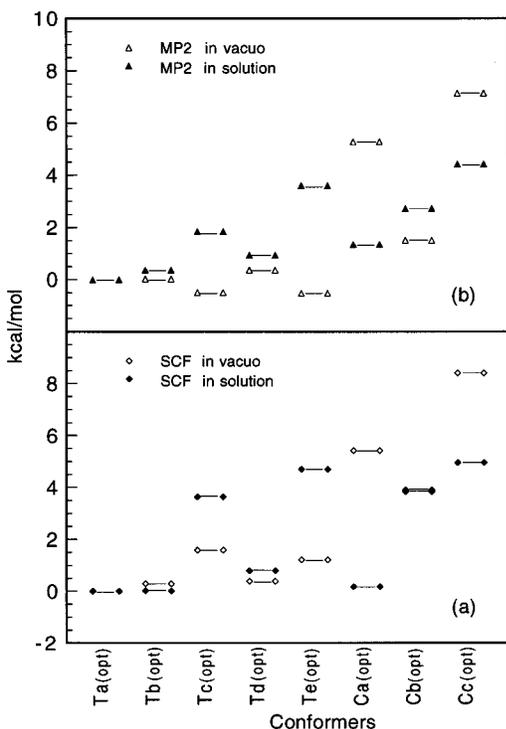
Stability of a Synthetic Dipeptide: PIDOTIMOD

J. Phys. Chem. A, Vol. 103, No. 29, 1999 **5831**

Figure 12. 6-31G* relative free energies (including G_{intra}) in vacuo (empty markers) and in aqueous solution (solid markers) for the lowest energy conformers fully optimized in vacuo (see text) with respect to Ta(opt), taken as zero, (a) at the HF level (diamonds) and (b) at the MP2 level (triangles).

less favorable than Ca (1.8 kcal/mol at the MP2 level). These results are not shown.

The addition of thermal corrections to the Gibbs free energy, computed in vacuo on the fully optimized structures, displayed in parts a and b of Figure 12, produces a slight adjustment (up to 0.25 kcal/mol) for Ta(opt), Td(opt), Ca(opt), and Tb(opt) in increasing order, with the largest change (which is however below 0.9 kcal/mol) still for Cb(opt). The intermediate adjustments are 0.45, 0.67, and 0.8 kcal/mol for Cc(opt), Te(opt), and Tc(opt), respectively.

By comparing Figure 12 to Figure 9, however, it is apparent that on the average the relative solvation free energies are more favorable for the structures in Figure 9, i.e., for structures not fully optimized in vacuo. Some of the lowest energy conformers in vacuo, in fact, present an intramolecular H-bond which prevents an effective interaction with water, because the polar groups involved in it are no longer available to interact with the solvent; these conformers should presumably undergo conformational changes in solution. Therefore, the best strategy of course would be to carry out geometry optimizations in solution, but this is computationally expensive especially when a conformational search is supposed to be necessary.

In this kind of system, in our opinion it is convenient to consider a rather large number of conformers and evaluate the solvent effect and the solvation free energy. Interestingly enough, the solvent effect sharply stabilizes the cis conformers over the trans ones both at the SCF and MP2 levels, though with the inclusion of DCR terms and thermal corrections the population of the cis conformers is either much lower (17% at the MP2 level) or much higher (66% at the HF level) than the experimental finding.

Conclusions

Several questions concerning the conformational preferences of PIDOTIMOD have been addressed in this paper, namely,

(a) the reliability of previous MM results through the determination of the $\phi_2 = 0°$ and $180°$ PES in the flexible rotor approximation both at the HF/STO-3G* and 6-31G* levels; (b) the inadequacy of the STO-3G* basis set which, for $\phi_2 = 180°$ and $120° \leq \phi_1 \leq 260°$, favors the nitrogen proton shuttling to the adjacent carboxyl anion, while a 13 kcal/mol barrier would prevent this process at the 6-31G* level; (c) the effect of correlation corrections at the MP2 level, which stabilize the structures presenting intramolecular H-bonds (Tc and Te); (d) the solvent effect evaluated in the PCM framework, both at the HF and MP2 levels, on stable conformers lying on the $\phi_2 = 0°$ or $180°$ PES, which favors the structures fully exposed to the solvent, and in particular stabilizes the cis conformers; (e) the trans−cis interconversion, which in vacuo should occur for $\phi_2 \approx 40°$, with a barrier of about 13 kcal/mol; (f) the influence of the pyramidalization of the thiazolidin ring N in determining the cis or trans conformation; (g) the substantially more favorable free energy of solvation obtained for structures not fully optimized in vacuo, which suggests either the use of optimizations in solution (when affordable) or the analysis of solvent effects in a rather wide choice of conformers.

The solvent effect shows a noticeable dependence not only on the solute geometry but also on the computational level (HF or MP2) which favors in turn either cis or trans conformers, respectively.

References and Notes

(1) Coppi, G.; Mailland, F. *Pharmacol. Res.* **1990**, *22*, 126.

(2) Smith Kendall, A. *Interleukin-2*; Academic Press: New York, 1988.

(3) Smith Kendall, A. *Annu. Rev. Cell Biol.* **1989**, *5*, 397.

(4) Villani, V.; Pucciariello, R.; Crimella, T.; Stradi, R. *J. Mol. Struct.* **1993**, *298*, 177.

(5) Villani, V.; Pucciariello, R. *J. Mol. Struct.* **1994**, *317*, 197.

(6) Frisch, M. J.; Trucks, G. W.; Schlegel, H. B.; Gill, P. M. W.; Johnson, B. G.; Robb, M. A.; Cheeseman, J. R.; Keith, T.; Petersson, G. A.; Montgomery, J. A.; Raghavachari, K.; Al-Laham, M. A.; Zakrzewski, V. G.; Ortiz, J. V.; Foresman, J. B.; Peng, C. Y.; Ayala, P. Y.; Chen, W.; Wong, M. W.; Andres, J. L.; Replogle, E. S.; Gomperts, R.; Martin, R. L.; Fox, D. J.; Binkley, J. S.; Defrees, D. J.; Baker, J.; Stewart, J. P.; Head-Gordon, M.; Gonzalez, C.; Pople, J. A. *Gaussian 94,* revision D.4; Gaussian, Inc.: Pittsburgh, PA, 1995.

(7) Collins, J. B.; Schleyer, P. v. R.; Binkley, J. S.; Pople, J. A. *J. Chem. Phys.* **1976**, *64*, 5142.

(8) Hehre, W. J.; Stewart, R. F.; Pople, J. A. *J. Chem. Phys.* **1969**, *51*, 2657.

(9) Hehre, W. J.; Ditchfield, R.; Pople, J. A. *J. Chem. Phys.* **1972**, *56*, 2257.

(10) Hariharan, P. C.; Pople, J. A. *Theor. Chim. Acta* **1973**, *28*, 213.

(11) Alkorta, I. *Theor. Chim. Acta* **1994**, *89*, 1.

(12) (a) Møller, C.; Plesset, M. S. *Phys. Rev.* **1934**, *46*, 618. (b) Pople, J. A.; Binkley, J. S.; Seeger, R. *Int. J. Quantum Chem.* **1976**, *10s*, 1. (c) Krishnan, R.; Frisch, M. J.; Pople, J. A. *J. Chem. Phys.* **1980**, *72*, 4244.

(13) Alagona, G.; Ghio, C.; Cammi, R.; Tomasi, J. *Int. J. Quantum Chem.* **1987**, *32*, 207.

(14) McQuarrie, D. *Statistical Mechanics*; Harper & Row: New York, 1976.

(15) Hehre, W. J.; Radom, L.; Schleyer, P. v. R.; Pople, J. A. *Ab Initio Molecular Orbital Theory*; Wiley: New York, 1986.

(16) Nagy, P.; Dunn, W. J., III; Alagona, G.; Ghio, C. *J. Am. Chem. Soc.* **1991**, *113*, 6719.

(17) Alagona, G.; Ghio, C. *J. Mol. Struct. (THEOCHEM)* **1992**, *254*, 287.

(18) (a) Alagona, G.; Cammi, R.; Ghio, C.; Tomasi, J. *Vestn. Slov. Kem. Drus.* **1987**, *34*, 149. (b) Alagona, G.; Ghio, C.; Cammi, R.; Tomasi, J. *Int. J. Quantum Chem.* **1987**, *32*, 207−226. (c) Alagona, G.; Ghio, C.; Cammi, R.; Tomasi, J. In *Molecules in Physics, Chemistry and Biology*; Maruani, J., Ed.; Topics in Molecular Organization and Engineering; Kluwer: Dordrecht, 1988; Vol. 2, p 507. (d) Alagona, G.; Cammi, R.; Ghio, C.; Tomasi, J. *Int. J. Quantum Chem.* **1989**, *35*, 223.

(19) (a) Alagona, G.; Ghio, C.; Kollman, P. A. *J. Am. Chem. Soc.* **1983**, *105*, 5226. (b) Alagona, G.; Ghio, C.; Tomasi, J. *J. Phys. Chem.* **1989**, *93*, 5401.

Alagona et al.

(20) (a) Scheiner, S.; Redfern, P.; Hillebrand, E. A. *Int. J. Quantum Chem.* **1986**, *29*, 817. (b) Frisch, M. J.; Del Bene, J. E.; Binkley, J. S.; Schaefer, H. F., III *J. Chem. Phys.* **1986**, *84*, 2279. (c) Del Bene, J. E. *J. Comput. Chem.* **1987**, *8*, 810. (d) Del Bene, J. E. *J. Phys. Chem.* **1988**, *92*, 2874.

(21) Li, G.-S.; Maigret, B.; Rinaldi, D.; Ruiz-López, M. F. *J. Comput. Chem.* **1998**, *19*, 1675.

(22) Tuñon, I.; Tortonda, F. R.; Pascual-Ahuir, J. L.; Silla, E. *J. Mol. Struct. (THEOCHEM)* **1996**, *371*, 117.

(23) Clark, T.; Chandrasekhar, J.; Spitznagel, G. W.; Schleyer, P. v. R. *J. Comput. Chem.* **1983**, *4*, 294.

(24) Alagona, G.; Ghio, C.; Giolitti, A.; Monti, S. *Theor. Chem. Acc.* **1999**, *101*, 143.

(25) (a) Miertus, S.; Scrocco, E.; Tomasi, J. *Chem. Phys.* **1981**, *55*, 117. (b) Bonaccorsi, R.; Cimiraglia, R.; Tomasi, J. *J. Comput. Chem.* **1983**, *4*, 567. (c) Bonaccorsi, R.; Cimiraglia, R.; Tomasi, J. *Chem. Phys. Lett.* **1983**, *99*, 77. (d) Pascual-Ahuir, J. L.; Silla, E.; Tomasi, J.; Bonaccorsi, R. *J. Comput. Chem.* **1987**, *8*, 778.

(26) Tomasi, J.; Persico, M. *Chem. Rev.* **1994**, *94*, 2027.

(27) Barone, V.; Cossi, M.; Tomasi, J. *J. Chem. Phys.* **1997**, *107*, 3210.

(28) Cammi, R.; Tomasi, J. *J. Chem. Phys.* **1994**, *100*, 7495.

(29) Mennucci, B.; Tomasi, J. *J. Chem. Phys.* **1997**, *106*, 5151.

(30) (a) Cossi, M.; Tomasi, J.; Cammi, R. *Int. J. Quantum Chem. Symp.* **1995**, *29*, 695. (b) Pierotti, R. A. *Chem. Rev.* **1976**, *76*, 717.

(31) Cossi, M.; Mennucci, B.; Cammi, R. *J. Comput. Chem.* **1996**, *17*, 57.

(32) Olivares del Valle, F. J.; Tomasi, J. *Chem. Phys.* **1991**, *150*, 139.